

# Electrically driven photon statistics engineering in quantum-dot circuit quantum electrodynamics


Lei-Lei Nian<sup>1,2</sup>, Bo Zheng<sup>1,3,4</sup> and Jing-Tao Lü<sup>2,\*</sup>

<sup>1</sup>*School of Physics and Astronomy, Yunnan University, Kunming 650091, People's Republic of China*

<sup>2</sup>*School of Physics, Institute for Quantum Science and Engineering, and Wuhan National High Magnetic Field Center, Huazhong University of Science and Technology, Wuhan 430074, People's Republic of China*

<sup>3</sup>*Department of Physics, Zhejiang University, Hangzhou 310027, People's Republic of China*

<sup>4</sup>*Collaborative Innovation Center of Advanced Microstructures, Nanjing University, Nanjing 210093, People's Republic of China*

 (Received 11 July 2022; revised 22 May 2023; accepted 31 May 2023; published 14 June 2023)

Circuit quantum electrodynamics (cQED) systems represent an important platform to study light-matter interaction at the nanoscale. However, an all-electrical scheme for photon statistics engineering in cQED, has so far not been established. Here, we propose a generation scheme of arbitrary photon statistics, based on current-driven joint interference effect in a three-body setup with one biased double quantum dot capacitively coupled to two microwave cavities. Antibunched, bunched, superthermal, and coherent photon emissions can be achieved and regulated by tuning inelastic electron tunneling processes. Generation of quantum correlation between cavities, indicated by the violation of classical Cauchy-Schwarz inequality, and quantum to classical transition can be further observed. Our scheme, proposed in a three-body cQED, can be extended toward many-body systems, as verified in a four-body setup.

DOI: [10.1103/PhysRevB.107.L241405](https://doi.org/10.1103/PhysRevB.107.L241405)

**Introduction.** Building hybrid circuit quantum electrodynamics (cQED) system by coupling micro- or nanoscale electrical circuit to cavity photons provides a versatile platform for the study of light-matter interaction at the fundamental level [1–12]. Understanding, generating, and manipulating various photon statistics based on such controllable cQED setups has potential applications in quantum information, quantum cryptography, quantum computing, and quantum simulation [13–16]. In a standard cQED setup, hereafter termed two-body cQED, with an electrical circuit coupled to one cavity, current-driven photon emissions with sub-Poissonian, Poissonian, or super-Poissonian statistics can be generated [17–22]. Going beyond the standard setup, realization of three-body cQED has triggered an immense interest for generating nonequilibrium correlation and entanglement, such as cavity-mediated electronic entanglement between two distant double quantum dots (QD) [23–28] and electron-transport-induced photonic entanglement between two cavities [29].

Due to this remarkable progress, such cQED platforms open up new directions for the exploration of nonequilibrium statistics of photons driven by electrical carrier injection in compact integrated devices, thereby avoiding the limitations of stability and scalability in bulk optical components [30]. However, unlike in quantum optical cavity QED, controlling photon statistics in cQED (such as QD-cQED and beyond) via single-electron tunneling still remains a challenge, hindered by the absence of the well-established conventional or unconventional photon blockade mechanism [31–36]. It is, therefore, desirable to develop an electrical scheme in cQED setup for engineering statistical properties of emitted photons.

In this Letter, we propose such an all-electrical scheme, which does not rely on strong electron-photon coupling and allows one to achieve different kinds of photon statistics with classical or quantum correlation. To be specific, we start from a three-body cQED system by coupling weakly one current-carrying double QD to two microwave cavities (Fig. 1), and find that the physics underlying this electrical scheme involves a joint interference effect between two photon-emission channels. Below, we will show that such a scheme is not only enough to generate the conventional photon statistics including antibunching, bunching, and coherent in two-body cQED systems [17–20,22,37–40], but it also has peculiar features that allow unexpected superthermal photon emission and quantum correlation. To further extend the possibilities for testing multi-degree-of-freedom photon statistics and quantum correlation, we generalize the scheme to many-body cQED setup.

Compared with existing schemes of controlling photon statistics in electrically driven two-body cQED devices [17–20,22,37–40], the proposed scheme is shown to enable generation of arbitrary photon statistics, which represents an analogous regime of the photon blockade via an electrical mean. As the electrical current can excite different photon degrees of freedom, the photonic quantum correlation and even quantum entanglement gained here may enrich the potential application of cQED devices in quantum information process.

**Model for three-body cQED setup.** We start from a three-body cQED setup where a current-driven double quantum dot (DQD) is capacitively coupled to two microwave cavities, as shown in Fig. 1. The system Hamiltonian is ( $\hbar = 1$ )

$$\begin{aligned} H_s &= H_d + H_{c1} + H_{c2}, \\ H_d &= \varepsilon_e d_e^\dagger d_e + \varepsilon_g d_g^\dagger d_g, \\ H_{ci} &= \omega_i a_i^\dagger a_i + g_i (a_i^\dagger d_g^\dagger d_e + a_i d_e^\dagger d_g), \end{aligned} \quad (1)$$

\*jtl@hust.edu.cn

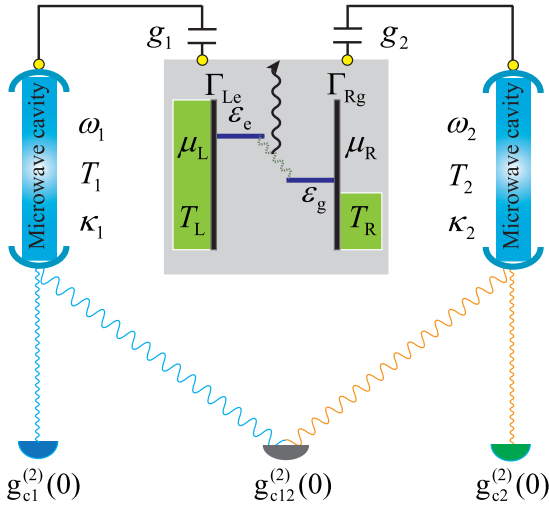


FIG. 1. Schematic of a three-body cQED system consisting of one current-driven DQD system and two microwave cavities. The two electronic levels  $\varepsilon_e$  and  $\varepsilon_g$  are coupled to two electrodes (L and R) with chemical potential  $\mu_{L,R}$  and temperature  $T_{L,R}$  at rates  $\Gamma_{Le}$  and  $\Gamma_{Rg}$ . The two microwave cavities with angular frequencies  $\omega_1$  and  $\omega_2$ , capacitively coupled to the DQD [41–48], are dissipated into two thermal baths with temperatures  $T_1$  and  $T_2$  at rates  $\kappa_1$  and  $\kappa_2$ . A bias voltage  $V_{LR} = (\mu_L - \mu_R)/e$  between electrodes drives the single-electron tunneling in the DQD, and thus the photon emissions of the cavities where their statistics are characterized by second-order correlation functions  $g_{c1}^{(2)}(0)$ ,  $g_{c2}^{(2)}(0)$ , and  $g_{c12}^{(2)}(0)$ . Depending on the Coulomb charging energy of the DQD ( $\sim 5$ meV), the bias voltage can be tuned by an external electric field from gigahertz to terahertz frequencies.

where  $H_d$  describes the isolated DQD, and  $d_e^\dagger$  ( $d_g^\dagger$ ) creates an electron of energy  $\varepsilon_e$  ( $\varepsilon_g$ ) on the level e (g). The first term in  $H_{ci}$  ( $i = 1, 2$ ) describes the cavity mode with creation (annihilation) operator  $a_i^\dagger$  ( $a_i$ ) and angular frequency  $\omega_i$ , while the second term, under rotating-wave approximation, characterizes the cavity excitation (de-excitation) by the inelastic tunneling electrons between levels e and g, where the electron-photon interaction is characterized by  $g_i$ .

We model the system dynamics using the Lindblad master equation [49–51]

$$\frac{d}{dt}\rho(t) = -i[H_s, \rho(t)] + \mathcal{D}_e[\rho(t)] + \sum_{i=1,2} \mathcal{D}_{ci}[\rho(t)], \quad (2)$$

where  $\rho(t)$  is the reduced density matrix of the system. The first term at the right hand side describes unitary evolution of the system. The second and third terms account for the dissipation due to coupling with the electrode and the thermal bath, which are  $\mathcal{D}_e[\rho(t)] = \sum_{\alpha=L,R} (\Gamma_{\alpha l \uparrow} \mathcal{D}[d_l^\dagger, \rho(t)] + \Gamma_{\alpha l \downarrow} \mathcal{D}[d_l, \rho(t)])$  and  $\mathcal{D}_{ci}[\rho(t)] = \kappa_{i \uparrow} \mathcal{D}[a_i^\dagger, \rho(t)] + \kappa_{i \downarrow} \mathcal{D}[a_i, \rho(t)]$ , where  $\alpha = L(R)$  for  $l = e(g)$ .  $\Gamma_{\alpha l \uparrow} = \Gamma_{\alpha l} f_v(\varepsilon_l)/2$  describes the electron tunneling from electrodes to central electronic states, while  $\Gamma_{\alpha l \downarrow} = \Gamma_{\alpha l} (1 - f_v(\varepsilon_l))/2$  is for the inverse process.  $\kappa_{i \uparrow} = \kappa_i n_B(\omega_i)/2$  and  $\kappa_{i \downarrow} = \kappa_i (1 + n_B(\omega_i))/2$  correspond, respectively, to the heating and cooling of the cavity mode induced by the coupling to the thermal bath.  $\Gamma_{\alpha l}$  is the level broadening function of the state  $l$  induced by the electrode  $\alpha$ . The Fermi-Dirac

distribution of the electrode  $\alpha$  with the chemical potential  $\mu_\alpha$  is denoted as  $f_\alpha(\varepsilon_l) = [e^{(\varepsilon_l - \mu_\alpha)/k_B T} + 1]^{-1}$ .  $\kappa_i$  is the dissipation rate of cavity and  $n_B(\omega_i) = [e^{\hbar\omega_i/k_B T} - 1]^{-1}$  is the equilibrium thermal occupation of the cavity photon. Finally,  $\mathcal{D}[O, \rho(t)] = 2O\rho(t)O^\dagger - O^\dagger O\rho(t) - \rho(t)O^\dagger O$  denotes the Lindblad superoperator with arbitrary operator  $O$ . We have taken the same temperature  $T$  for all degrees of freedom.

*Electrical engineering of photon statistics.* The statistical properties of cavity photons can be characterized by the equal-time second-order correlation functions  $g_{ci}^{(2)}(0) = \text{Tr}(\rho_{ss} a_i^\dagger a_i^\dagger a_i a_i) / [\text{Tr}(\rho_{ss} a_i^\dagger a_i)]^2$  and  $g_{c12}^{(2)}(0) = \text{Tr}(\rho_{ss} a_1^\dagger a_2^\dagger a_2 a_1) / [\text{Tr}(\rho_{ss} a_1^\dagger a_1) \text{Tr}(\rho_{ss} a_2^\dagger a_2)]$ , where  $\rho_{ss}$  is the steady-state density matrix of  $\rho(t)$  (Appendix A [52]). Our goal is to electrically engineer statistical properties of emitted photons, resulting from an interplay between two outputs. To achieve this, we introduce a unitary transformation [53,54]

$$a_1 = b_1 \cos \theta + b_2 \sin \theta, \quad (3)$$

$$a_2 = b_2 \cos \theta - b_1 \sin \theta. \quad (4)$$

The system Hamiltonian can then be rewritten as

$$\tilde{H}_s = \tilde{H}_d + \tilde{H}_{c1} + \tilde{H}_{c2} + \tilde{H}_{c12}, \quad (5)$$

where  $\tilde{H}_d = H_d$  and

$$\tilde{H}_{ci} = \tilde{\omega}_i b_i^\dagger b_i + \tilde{g}_i (b_i^\dagger d_e^\dagger + b_i d_e^\dagger), \quad (6)$$

$$\tilde{H}_{c12} = \tilde{g}_{12} (b_1^\dagger b_2 + b_2^\dagger b_1). \quad (7)$$

Here  $\tilde{\omega}_1 = \omega_1 \cos^2 \theta + \omega_2 \sin^2 \theta$ ,  $\tilde{\omega}_2 = \omega_1 \sin^2 \theta + \omega_2 \cos^2 \theta$ ,  $\tilde{g}_1 = g_1 \cos \theta - g_2 \sin \theta$ ,  $\tilde{g}_2 = g_1 \sin \theta + g_2 \cos \theta$ , and  $\tilde{g}_{12} = \sin 2\theta (\omega_1 - \omega_2)/2$  are the renormalized angular frequencies and coupling parameters. The corresponding master equation takes a similar form with Eq. (2), except for a joint dissipation  $\tilde{\mathcal{D}}_{c12}[\tilde{\rho}(t)] = \sum_{i \neq j} \tilde{\kappa}_{i \uparrow} [2b_i^\dagger \tilde{\rho}(t) b_j - b_j^\dagger b_i^\dagger \tilde{\rho}(t) - \tilde{\rho}(t) b_j b_i^\dagger] + \sum_{i \neq j} \tilde{\kappa}_{i \downarrow} [2b_i \tilde{\rho}(t) b_j^\dagger - b_i^\dagger b_j \tilde{\rho}(t) - \tilde{\rho}(t) b_i^\dagger b_j]$  with  $\tilde{\kappa}_{12\sigma} = \tilde{\kappa}_{21\sigma} = \sin 2\theta (\kappa_{1\sigma} - \kappa_{2\sigma})/2$  ( $\sigma = \uparrow, \downarrow$ ), where  $\tilde{\rho}(t)$  is the density matrix in the normal-mode basis. The emission statistics of modes  $b_1$  and  $b_2$  are characterized by  $\tilde{g}_{ci}^{(2)}(0) = \text{Tr}(\tilde{\rho}_{ss} b_i^\dagger b_i^\dagger b_i b_i) / [\text{Tr}(\tilde{\rho}_{ss} b_i^\dagger b_i)]^2$  and  $\tilde{g}_{c12}^{(2)}(0) = \text{Tr}(\tilde{\rho}_{ss} b_1^\dagger b_2^\dagger b_2 b_1) / [\text{Tr}(\tilde{\rho}_{ss} b_1^\dagger b_1) \text{Tr}(\tilde{\rho}_{ss} b_2^\dagger b_2)]$ , where  $\tilde{\rho}_{ss}$  is the steady-state form of  $\tilde{\rho}(t)$  (Appendix B [52]).

The canonical transformations allow us to eliminate the second term of the interaction Hamiltonian  $\tilde{H}_{c2}$  by taking  $\tilde{g}_2 = 0$  and thus  $\theta = \arctan(-g_2/g_1)$ . In comparison with Eq. (2), modes  $b_1$  and  $b_2$  evolve under two additional actions, indicating by a direct coupling  $\tilde{H}_{c12}$  and a collective dissipation  $\tilde{\mathcal{D}}_{c12}[\tilde{\rho}(t)]$ . The second-order correlation functions of modes  $a_1$  and  $a_2$  are therefore given by

$$g_{c1}^{(2)}(0) = \frac{\mathcal{G}_1^\dagger + \mathcal{G}_{12}^\dagger + \mathcal{G}_2^\dagger}{(\mathcal{N}_1^\dagger + \mathcal{N}_{12} + \mathcal{N}_2^\dagger)^2}, \quad (8)$$

$$g_{c2}^{(2)}(0) = \frac{\mathcal{G}_1^\top + \mathcal{G}_{12}^\top + \mathcal{G}_2^\top}{(\mathcal{N}_1^\top - \mathcal{N}_{12} + \mathcal{N}_2^\top)^2}, \quad (9)$$

where  $\mathcal{G}_i^\dagger$  ( $\mathcal{G}_i^\top$ ) and  $\mathcal{N}_i^\dagger$  ( $\mathcal{N}_i^\top$ ) are the  $\theta$ -dependent fourth- and second-order autocorrelation functions of modes  $b_1$  and  $b_2$ , while  $\mathcal{G}_{12}^\dagger$ ,  $\mathcal{G}_{12}^\top$ , and  $\mathcal{N}_{12}$  are cross correlations. The detailed expressions are displayed in Appendix C [52]. Clearly,

the destructive or constructive interference can be achieved depending on the signs of  $\mathcal{G}_{12}^{\perp}$ ,  $\mathcal{G}_{12}^{\top}$ , and  $\mathcal{N}_{12}$ . Therefore, the joint interference effect between modes  $b_1$  and  $b_2$  can be used to engineer the photon statistics of modes  $a_1$  and  $a_2$ .

For  $\omega_1 = \omega_2$ ,  $g_1 = g_2$ , and  $\kappa_1 = \kappa_2$ , modes  $a_1$  and  $a_2$  share the same statistics with  $g_{c1}^{(2)}(0) = g_{c2}^{(2)}(0)$  as indicated by Eq. (2), while the statistical distribution cannot be shown explicitly. In the normal-mode basis,  $\tilde{H}_{c12} = 0$  and  $\tilde{\mathcal{D}}_{c12}[\tilde{\rho}(t)] = 0$ , which yields  $\tilde{g}_{c12}^{(2)}(0) = 1$  and

$$g_{ci}^{(2)}(0) = [\text{Tr}(\tilde{\rho}_{ss} b_1^{\dagger} b_1^{\dagger} b_1 b_1) + \text{Tr}(\tilde{\rho}_{ss} b_2^{\dagger} b_2^{\dagger} b_2 b_2) + 4\text{Tr}(\tilde{\rho}_{ss} b_1^{\dagger} b_1) \text{Tr}(\tilde{\rho}_{ss} b_2^{\dagger} b_2)] \times [\text{Tr}(\tilde{\rho}_{ss} b_1^{\dagger} b_1) + \text{Tr}(\tilde{\rho}_{ss} b_2^{\dagger} b_2)]^{-2}, \quad (10)$$

where the mode  $b_2$  is solely coupled to a thermal bath, and consequently, it is in thermal state with  $\tilde{g}_{c2}^{(2)}(0) = 2$ . Then the emission statistics of modes  $a_1$  and  $a_2$  can be verified to follow the mode  $b_1$  excited by the biased DQD and a thermal bath, where  $g_{ci}^{(2)}(0)$  is equal to the modified  $\tilde{g}_{ci}^{(2)}(0)$  (Appendix C [52]). Thus, one cannot generate the photon statistics other than the mode  $b_1$  when the two cavities gain the same energy from the inelastic current. In such a case, the current-driven correlation between modes  $b_1$  and  $b_2$  cannot be established, and thus the joint interference effect vanishes. Having established such a rule, we will focus on the regime with the interference effect induced by  $\tilde{H}_{c12} \neq 0$ ,  $\tilde{\mathcal{D}}_{c12}[\tilde{\rho}(t)] \neq 0$ , or both. To fulfill potential applications of our scheme in quantum information processing, we proceed by generating target photon statistics and quantum correlations.

*Cavity photon statistics.* For one cavity coupled to the biased DQD,  $g_1 = 0$  or  $g_2 = 0$ , at given applied voltage bias, an extra electron can only tunnel into the upper level from left electrode, relax to the lower level by the emission of one photon, and then tunnel out into right electrode. Thus, the emission statistics of the cavity is driven by the single electron transport [55–57], and the bath-induced thermalization can further yield  $g_{c1}^{(2)}(0) \in [0, 2]$  or  $g_{c2}^{(2)}(0) \in [0, 2]$ . However, such statistical upper limit can be breached by introducing an additional cavity, where the emission statistics of the modes  $a_1$  and  $a_2$  are involved in a joint interference effect between the normal modes  $b_1$  and  $b_2$ . Our proposal can be realized in extended two-body quantum dot cQED systems experimentally [1, 8, 58–62], and the parameters are estimated based on such experiments. The parameters of the quantum dots can be tuned *in situ* [63–66], including the energy-level structure, tunneling rates, and coupling strength.

Numerically, Fig. 2(a) shows the second-order correlation functions  $g_{c1}^{(2)}(0)$ ,  $g_{c2}^{(2)}(0)$ , and  $g_{c12}^{(2)}(0)$  versus chemical potential  $\mu_L$ . For  $\mu_L < \varepsilon_e$  where no electrons can tunnel from the left electrode to the high level, electron transport is blocked, such that the cavities are in thermal states. Hereafter, we focus on situations where this blocking is lifted. It is shown that the current-driven DQD coupled to single cavity yields antibunched, bunched, or coherent photon emission ( $g_{ci}^{(2)}(0) \leq 2$ ) depending on  $\mu_L$ , as indicated by the occupation probabilities  $p(m)$  and  $p(n)$  in Figs. 2(b) and 2(c). The current-driven DQD interacting with two cavities allows superthermal photon emission from mode  $a_2$  ( $g_{c2}^{(2)}(0) > 2$ ), which never occurs in single cavity case. We attribute these

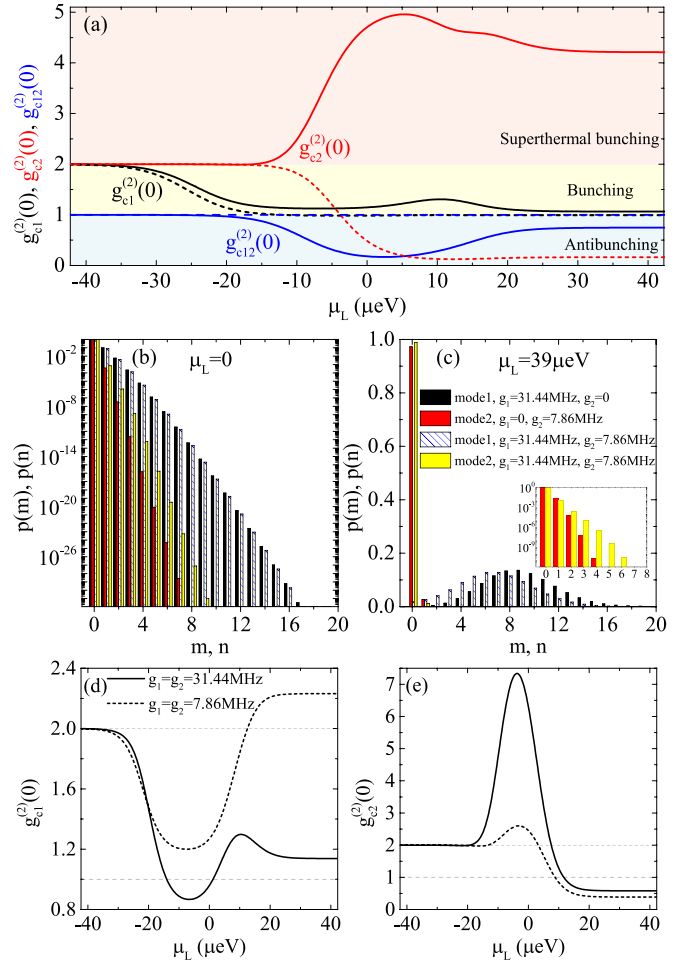


FIG. 2. (a) Second-order correlation functions  $g_{c1}^{(2)}(0)$ ,  $g_{c2}^{(2)}(0)$ , and  $g_{c12}^{(2)}(0)$  as a function of the chemical potential  $\mu_L$  with  $\omega_1 = 7.86 \text{ GHz}$  and  $\omega_2 = 7.8993 \text{ GHz}$ . The dashed lines for  $g_{c1}^{(2)}(0)$  with  $g_1 = 31.44 \text{ MHz}$  and  $g_2 = 0$  (black),  $g_{c2}^{(2)}(0)$  with  $g_1 = 0$  and  $g_2 = 7.86 \text{ MHz}$  (red), and  $g_{c12}^{(2)}(0)$  with  $g_1 = 0$  or  $g_2 = 0$  (blue). Similar to the dashed lines, the solid lines for  $g_1 = 31.44 \text{ MHz}$  and  $g_2 = 7.86 \text{ MHz}$ . (b) and (c) Occupation probabilities  $p(m)$  and  $p(n)$  of the cavity modes for  $\mu_L = 0$  and  $\mu_L = 39 \mu\text{eV}$ . The inset in (c) is an enlarged plot of  $\text{Log}_{10}[p(n)]$ . (d) and (e) Second-order correlation functions  $g_{c1}^{(2)}(0)$  and  $g_{c2}^{(2)}(0)$  as a function of the chemical potential  $\mu_L$  for  $g_1 = g_2 = 31.44 \text{ MHz}$  (solid line) and  $g_1 = 31.44 \text{ MHz}$ ,  $g_2 = 7.86 \text{ MHz}$  (dashed line) with  $\omega_1 = \omega_2 = 7.86 \text{ GHz}$ . Parameters:  $\varepsilon_e = 3.93 \text{ GHz}$ ,  $\varepsilon_g = -3.93 \text{ GHz}$ ,  $\Gamma_{Le} = 7.86 \text{ MHz}$ ,  $\Gamma_{Rg} = 1.572 \text{ MHz}$ ,  $\kappa_1 = 0.0786 \text{ MHz}$ ,  $\kappa_2 = 15.72 \text{ MHz}$ ,  $\mu_R = -97.5 \mu\text{eV}$ , and  $T = 384 \text{ mK}$ . Note that our results still hold even beyond the rotating-wave approximation (Appendix D [52]).

unexpected photon statistics to the current-driven joint interference effect induced by  $\tilde{H}_{c12} \neq 0$  and  $\tilde{\mathcal{D}}_{c12}[\tilde{\rho}(t)] \neq 0$ . For  $\mu_L = 0$ , the two cavities can be excited by the current induced by thermal broadening of Fermi-Dirac distribution, where the joint interference with  $\mathcal{G}_{12}^{\perp} < 0$  and  $\mathcal{N}_{12} > 0$  in Eq. (9) leads in fact to the superthermal photon emission from mode  $a_2$ . For  $\mu_L = 39 \mu\text{eV}$ , the cavities can be excited more effectively, while the superthermal photon statistics of mode  $a_2$  share the same mechanism with  $\mu_L = 0$ . To highlight the contribution of the collective dissipation  $\tilde{\mathcal{D}}_{c12}[\tilde{\rho}(t)] \neq 0$

induced by  $\kappa_1 \neq \kappa_2$  to the joint interference effect, the optimized dissipation rates are used. Taking the realistic experimental parameters with  $\kappa_1 = 2$  MHz [61] and  $\kappa_2 = 8$  MHz [59], the superthermal photon bunching with  $g_{c2}^{(2)}(0) \approx 3.78$  at  $\mu_L = 39$   $\mu\text{eV}$  is achieved for  $g_1 = 70.74$  MHz. Without the joint interference effect induced by  $\tilde{H}_{c12} = 0$  and  $\tilde{D}_{c12}[\tilde{\rho}(t)] = 0$ , the emissions of modes  $a_1$  and  $a_2$  behave qualitatively similar to mode  $b_1$  with the photon statistics of antibunching, bunching, or coherent (Appendix C [52]). In principle, the superthermal photon correlations can provide an effective way for improving phase sensitivity in interferometry measurements [67], detecting subwavelength interference [68], and reconstructing the photon number distributions [69] from gigahertz to terahertz frequencies in the electrically driven quantum dot cQED. Moreover, the superthermal intensity fluctuations allow other potential applications without optical nonlinear responses, such as two-photon luminescence microscopy [70] and thermal ghost imaging [71]. We note that a similar superthermal photon bunching can be achieved in quantum-dot-based bimodal micro- and nanolasers [72–78]. Furthermore, current-driven strong anticorrelation can be generated ( $g_{c12}^{(2)}(0) \ll 1$ ).

Next, we consider that the two cavities with asymmetric losses are excited symmetrically,  $\omega_1 = \omega_2$ ,  $g_1 = g_2$ , and  $\kappa_1 \neq \kappa_2$ , such that the direct mode-mode coupling vanishes  $\tilde{H}_{c12} = 0$ . In this case, the joint interference effect is solely dominated by the collective dissipation  $\tilde{D}_{c12}[\tilde{\rho}(t)]$ . The resulting photon statistics of the cavities  $g_{c1}^{(2)}(0)$  and  $g_{c2}^{(2)}(0)$  are shown in Figs. 2(d) and 2(e), respectively. For  $g_1 = g_2 = 31.44$  MHz, the emission statistics of mode  $a_1$  ( $a_2$ ) exhibits a transition from antibunching (superthermal bunching) to bunching (antibunching) by tuning  $\mu_L$ . A similar effect can be observed for  $g_1 = g_2 = 7.86$  MHz, where tuning  $\mu_L$  filters either photon bunching (superthermal bunching) or superthermal bunching (antibunching). Our setup can then generate desired photon statistics with an obvious switching effect, which may be used to design a photon filter, resulting from the voltage-mediated joint interference effect.

**Quantum correlation.** Another important property of the three-body cQED system is the current-driven correlation between the cavities. Normally, a classical two-mode correlation can be characterized by the well-known Cauchy-Schwarz inequality [79]

$$E_{CS} = \frac{\text{Tr}(\rho_{ss} a_1^\dagger a_2^\dagger a_2 a_1)}{\sqrt{\text{Tr}(\rho_{ss} a_1^\dagger a_1^\dagger a_1 a_1)} \sqrt{\text{Tr}(\rho_{ss} a_2^\dagger a_2^\dagger a_2 a_2)}} \leq 1, \quad (11)$$

where  $E_{CS}$  is the dimensionless Cauchy-Schwarz parameter,  $E_{CS} > 1$  yields the quantum correlation. Notice that  $E_{CS} = g_{c12}^{(2)}(0) / \sqrt{g_{c1}^{(2)}(0)g_{c2}^{(2)}(0)}$ , where  $E_{CS} \leq 1$  can be found without the joint interference effect (Appendix C [52]). We mention that the classical Cauchy-Schwarz inequality ( $E_{CS} \leq 1$ ) always holds in Fig. 2, thus building a classical correlation. In Fig. 3(a), we show the results for a large cavity dissipation at rate  $\kappa_1 = 157.2$  MHz, so the emission from the two cavities is dominated by the antibunched photons, and the generated photons are anticorrelated strongly with each other. Note that, the violation of the classical Cauchy-Schwarz inequality can be obtained,  $E_{CS} > 1$ , thus building a quantum correlation,

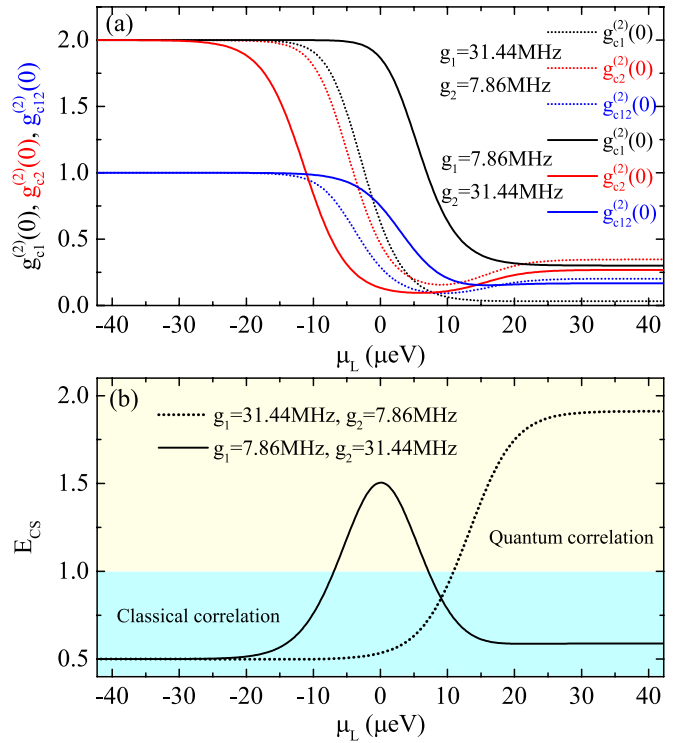


FIG. 3. (a) Second-order correlation functions  $g_{c1}^{(2)}(0)$ ,  $g_{c2}^{(2)}(0)$ , and  $g_{c12}^{(2)}(0)$  as a function of the chemical potential  $\mu_L$  for  $\kappa_1 = 157.2$  MHz, the dashed lines for  $g_1 = 31.44$  MHz and  $g_2 = 7.86$  MHz, the solid lines for  $g_1 = 7.86$  MHz and  $g_2 = 31.44$  MHz. (b) Similar to (a), but for Cauchy-Schwarz parameter  $E_{CS}$  versus  $\mu_L$ . The other parameters as in Fig. 2(d).

as presented in Fig. 3(b). Moreover, one can prove that the quantum entanglement can be created in such a quantum correlation (Appendix E [52]). Switching the electron-photon

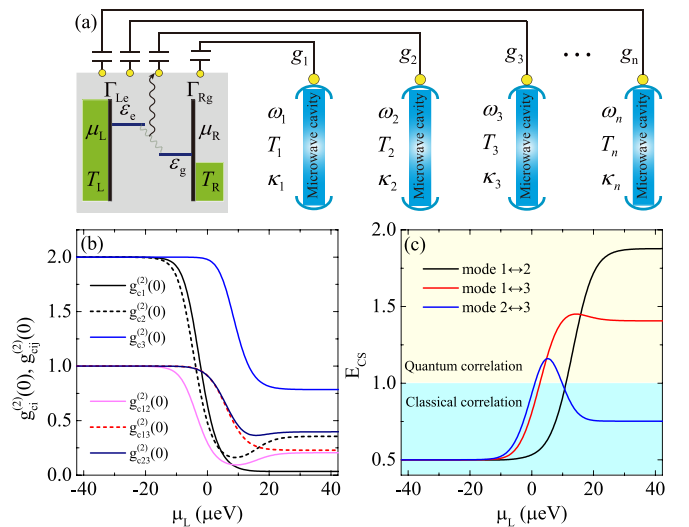


FIG. 4. (a) Sketch of the setup for a many-body quantum dot cQED system. (b) Second-order correlation functions  $g_{c1}^{(2)}(0)$  and  $g_{c2}^{(2)}(0)$  as a function of the chemical potential  $\mu_L$  for  $\omega_3 = 7.86$  GHz,  $g_3 = 11.79$  MHz, and  $\kappa_3 = 393$  MHz. (c) Similar to (b), but for Cauchy-Schwarz parameter  $E_{CS}$  versus  $\mu_L$ . The other parameters are the same as the dashed line in Fig. 3(b).

couplings, the behavior of  $E_{CS}$  around  $-9.75 \mu\text{eV} < \mu_L < 9.75 \mu\text{eV}$ , displays a quantum-classical transition. Again, this is a consequence of current-driven joint interference effect.

*Many-body cQED system.* Finally, we stress that the proposal can be applied to many-body cases [Fig. 4(a)]. As an example, we consider a four-body setup consisting of one current-driven DQD and three cavities. The Hamiltonian and master equation are obtained by setting  $i$  in Eqs. (1) and (2) up to 3. The four-body cQED system extends the possibilities for testing multi-degree-of-freedom photon statistics and quantum correlations, as shown in Figs. 4(b) and 4(c). As expected, the quantum correlation between arbitrary two cavities with photon antibunching and anticorrelation can be established, and the classical-to-quantum transition is observed. Furthermore, a regime with  $E_{CS} > 1$  for all pairs of modes simultaneously can be achieved (Appendix F [52]).

In principle, it is complicated to characterize the quantum correlation in many-body cQED systems, since the correlation between more than two cavities occurs in different inequivalent ways. In such a case, the multipartite-correlation criterion may be required, such as geometric correlation [80], global

correlation [81], and genuine multipartite correlation [82]. Note that, the quantum-to-classical transition may occur with increasing the cavities and complexity of the system, where it is challenging to capture the quantum correlation and quantum statistics.

*Summary.* We have shown that three-body cQED devices consisting of one biased double quantum dot and two microwave cavities can be used to engineer photon statistics. Based on current-driven joint interference effect, we proposed an all-electrical scheme to generate arbitrary photon statistics, including antibunching, bunching, superthermal bunching, and coherent. By tuning the bias voltage, classical or quantum correlation between cavities can be achieved, and that classical-to-quantum transition is possible. Moreover, extensions to a four-body cQED setup enable application of the proposal in many-body cQED systems.

*Acknowledgments.* This work has been funded by the National Natural Science Foundation of China (Grants No. 21873033, No. 12204405, No. 22273029, No. 12175193, and No. 11775186) and by the Yunnan Fundamental Research Project (Grant No. 202301AT070108).

- 
- [1] A. Stockklauser, V. F. Maisi, J. Basset, K. Cujia, C. Reichl, W. Wegscheider, T. Ihn, A. Wallraff, and K. Ensslin, Microwave Emission from Hybridized States in a Semiconductor Charge Qubit, *Phys. Rev. Lett.* **115**, 046802 (2015).
- [2] M. J. Gullans, Y.-Y. Liu, J. Stehlik, J. R. Petta, and J. M. Taylor, Phonon-Assisted Gain in a Semiconductor Double Quantum Dot Maser, *Phys. Rev. Lett.* **114**, 196802 (2015).
- [3] L. E. Bruhat, J. J. Viennot, M. C. Dartiailh, M. M. Desjardins, T. Kontos, and A. Cottet, Cavity Photons as a Probe for Charge Relaxation Resistance and Photon Emission in a Quantum Dot Coupled to Normal and Superconducting Continua, *Phys. Rev. X* **6**, 021014 (2016).
- [4] H. Imada, K. Miwa, M. Imai-Imada, S. Kawahara, K. Kimura, and Y. Kim, Single-Molecule Investigation of Energy Dynamics in a Coupled Plasmon-Exciton System, *Phys. Rev. Lett.* **119**, 013901 (2017).
- [5] L. Zhang, Y.-J. Yu, L.-G. Chen, Y. Luo, B. Yang, F.-F. Kong, G. Chen, Y. Zhang, Q. Zhang, Y. Luo, J.-L. Yang, Z.-C. Dong, and J. G. Hou, Electrically driven single-photon emission from an isolated single molecule, *Nat. Commun.* **8**, 580 (2017).
- [6] X. Mi, J. Cady, D. Zajac, P. Deelman, and J. R. Petta, Strong coupling of a single electron in silicon to a microwave photon, *Science* **355**, 156 (2017).
- [7] Y.-Y. Liu, J. Stehlik, C. Eichler, X. Mi, T. R. Hartke, M. J. Gullans, J. M. Taylor, and J. R. Petta, Threshold Dynamics of a Semiconductor Single Atom Maser, *Phys. Rev. Lett.* **119**, 097702 (2017).
- [8] T. R. Hartke, Y.-Y. Liu, M. J. Gullans, and J. R. Petta, Microwave Detection of Electron-Phonon Interactions in a Cavity-Coupled Double Quantum Dot, *Phys. Rev. Lett.* **120**, 097701 (2018).
- [9] M. Parzefall and L. Novotny, Optical antennas driven by quantum tunneling: A key issues review, *Rep. Prog. Phys.* **82**, 112401 (2019).
- [10] J. Lu, R. Wang, J. Ren, M. Kulkarni, and J.-H. Jiang, Quantum-dot circuit-QED thermoelectric diodes and transistors, *Phys. Rev. B* **99**, 035129 (2019).
- [11] R. Gutzler, M. Garg, C. R. Ast, K. Kuhnke, and K. Kern, Light-matter interaction at atomic scales, *Nat. Rev. Phys.* **3**, 441 (2021).
- [12] A. Blais, A. L. Grimsmo, S. M. Girvin, and A. Wallraff, Circuit quantum electrodynamics, *Rev. Mod. Phys.* **93**, 025005 (2021).
- [13] P. Kok, W. J. Munro, K. Nemoto, T. C. Ralph, J. P. Dowling, and G. J. Milburn, Linear optical quantum computing with photonic qubits, *Rev. Mod. Phys.* **79**, 135 (2007).
- [14] A. Aspuru-Guzik and P. Walther, Photonic quantum simulators, *Nat. Phys.* **8**, 285 (2012).
- [15] T. Northup and R. Blatt, Quantum information transfer using photons, *Nat. Photonics* **8**, 356 (2014).
- [16] A. Blais, S. M. Girvin, and W. D. Oliver, Quantum information processing and quantum optics with circuit quantum electrodynamics, *Nat. Phys.* **16**, 247 (2020).
- [17] N. Lambert, F. Nori, and C. Flindt, Bistable Photon Emission from a Solid-State Single-Atom Laser, *Phys. Rev. Lett.* **115**, 216803 (2015).
- [18] Y.-Y. Liu, T. R. Hartke, J. Stehlik, and J. R. Petta, Phase locking of a semiconductor double-quantum-dot single-atom maser, *Phys. Rev. A* **96**, 053816 (2017).
- [19] G. Rastelli and M. Governale, Single atom laser in normal-superconductor quantum dots, *Phys. Rev. B* **100**, 085435 (2019).
- [20] M. Mantovani, A. D. Armour, W. Belzig, and G. Rastelli, Dynamical multistability in a quantum-dot laser, *Phys. Rev. B* **99**, 045442 (2019).
- [21] Q. Schaefferbeke, R. Avriller, T. Frederiksen, and F. Pistolesi, Single-Photon Emission Mediated by Single-Electron Tunneling in Plasmonic Nanojunctions, *Phys. Rev. Lett.* **123**, 246601 (2019).

- [22] L.-L. Nian, T. Wang, Z.-Q. Zhang, J.-S. Wang, and J.-T. Lü, Effective control of photon statistics from electroluminescence by fano-like interference effect, *J. Phys. Chem. Lett.* **11**, 8721 (2020).
- [23] N. Lambert, C. Flindt, and F. Nori, Photon-mediated electron transport in hybrid circuit-QED, *EPL (Europhysics Letters)* **103**, 17005 (2013).
- [24] L. D. Contreras-Pulido, C. Emary, T. Brandes, and R. Aguado, Non-equilibrium correlations and entanglement in a semiconductor hybrid circuit-QED system, *New J. Phys.* **15**, 095008 (2013).
- [25] C. Bergenfeldt and P. Samuelsson, Nonlocal transport properties of nanoscale conductor-microwave cavity systems, *Phys. Rev. B* **87**, 195427 (2013).
- [26] C. Bergenfeldt, P. Samuelsson, B. Sothmann, C. Flindt, and M. Büttiker, Hybrid Microwave-Cavity Heat Engine, *Phys. Rev. Lett.* **112**, 076803 (2014).
- [27] G.-W. Deng, D. Wei, S.-X. Li, J. Johansson, W.-C. Kong, H.-O. Li, G. Cao, M. Xiao, G.-C. Guo, F. Nori, H.-W. Jiang, and G.-P. Guo, Coupling two distant double quantum dots with a microwave resonator, *Nano Lett.* **15**, 6620 (2015).
- [28] G. Nicolí, M. S. Ferguson, C. Rössler, A. Wolfertz, G. Blatter, T. Ihn, K. Ensslin, C. Reichl, W. Wegscheider, and O. Zilberberg, Cavity-Mediated Coherent Coupling between Distant Quantum Dots, *Phys. Rev. Lett.* **120**, 236801 (2018).
- [29] F. Hellbach, F. Pauly, W. Belzig, and G. Rastelli, Quantum-correlated photons generated by nonlocal electron transport, *Phys. Rev. B* **105**, L241407 (2022).
- [30] J. L. O'Brien, Optical quantum computing, *Science* **318**, 1567 (2007).
- [31] K. M. Birnbaum, A. Boca, R. Miller, A. D. Boozer, T. E. Northup, and H. J. Kimble, Photon blockade in an optical cavity with one trapped atom, *Nature (London)* **436**, 87 (2005).
- [32] T. C. H. Liew and V. Savona, Single Photons from Coupled Quantum Modes, *Phys. Rev. Lett.* **104**, 183601 (2010).
- [33] M. Bamba, A. Imamoğlu, I. Carusotto, and C. Ciuti, Origin of strong photon antibunching in weakly nonlinear photonic molecules, *Phys. Rev. A* **83**, 021802(R) (2011).
- [34] A. Majumdar, M. Bajcsy, A. Rundquist, and J. Vučković, Loss-Enabled Sub-Poissonian Light Generation in a Bimodal Nanocavity, *Phys. Rev. Lett.* **108**, 183601 (2012).
- [35] H. Flayac and V. Savona, Unconventional photon blockade, *Phys. Rev. A* **96**, 053810 (2017).
- [36] H. J. Sniijders, J. A. Frey, J. Norman, H. Flayac, V. Savona, A. C. Gossard, J. E. Bowers, M. P. van Exter, D. Bouwmeester, and W. Löffler, Observation of the Unconventional Photon Blockade, *Phys. Rev. Lett.* **121**, 043601 (2018).
- [37] P.-Q. Jin, M. Marthaler, J. H. Cole, A. Shnirman, and G. Schön, Lasing and transport in a quantum-dot resonator circuit, *Phys. Rev. B* **84**, 035322 (2011).
- [38] T. L. van den Berg and P. Samuelsson, Charge-photon transport statistics and short-time correlations in a single quantum dot-resonator system with an arbitrarily large coupling parameter, *Phys. Rev. B* **100**, 035408 (2019).
- [39] B. K. Agarwalla, M. Kulkarni, and D. Segal, Photon statistics of a double quantum dot micromaser: Quantum treatment, *Phys. Rev. B* **100**, 035412 (2019).
- [40] S. M. Tabatabaie and N. Jahangiri, Lasing in a coupled hybrid double quantum dot-resonator system, *Phys. Rev. B* **101**, 115135 (2020).
- [41] M. Mariantoni, F. Deppe, A. Marx, R. Gross, F. K. Wilhelm, and E. Solano, Two-resonator circuit quantum electrodynamics: A superconducting quantum switch, *Phys. Rev. B* **78**, 104508 (2008).
- [42] F. W. Strauch, K. Jacobs, and R. W. Simmonds, Arbitrary Control of Entanglement between two Superconducting Resonators, *Phys. Rev. Lett.* **105**, 050501 (2010).
- [43] C.-P. Yang, Q.-P. Su, S.-B. Zheng, and S. Han, Generating entanglement between microwave photons and qubits in multiple cavities coupled by a superconducting qutrit, *Phys. Rev. A* **87**, 022320 (2013).
- [44] M. Hua, M.-J. Tao, and F.-G. Deng, Universal quantum gates on microwave photons assisted by circuit quantum electrodynamics, *Phys. Rev. A* **90**, 012328 (2014).
- [45] A. Baust, E. Hoffmann, M. Haeberlein, M. J. Schwarz, P. Eder, J. Goetz, F. Wulschner, E. Xie, L. Zhong, F. Quijandria, B. Peropadre, D. Zueco, J.-J. Garcia Ripoll, E. Solano, K. Fedorov, E. P. Menzel, F. Deppe, A. Marx, and R. Gross, Tunable and switchable coupling between two superconducting resonators, *Phys. Rev. B* **91**, 014515 (2015).
- [46] C.-P. Yang, Q.-P. Su, S.-B. Zheng, and F. Nori, Crosstalk-insensitive method for simultaneously coupling multiple pairs of resonators, *Phys. Rev. A* **93**, 042307 (2016).
- [47] O. Kyriienko and A. S. Sørensen, Continuous-Wave Single-Photon Transistor Based on a Superconducting Circuit, *Phys. Rev. Lett.* **117**, 140503 (2016).
- [48] J. Zheng, J. Peng, P. Tang, F. Li, and N. Tan, Unified generation and fast emission of arbitrary single-photon multimode  $W$  states, *Phys. Rev. A* **105**, 062408 (2022).
- [49] G. Lindblad, On the generators of quantum dynamical semi-groups, *Commun. Math. Phys.* **48**, 119 (1976).
- [50] H.-P. Breuer and F. Petruccione, *The Theory of Open Quantum Systems* (Oxford University Press on Demand, 2002).
- [51] H. J. Carmichael, *Statistical Methods in Quantum Optics I: Master Equations and Fokker-Planck Equations* (Springer Science & Business Media, 2013).
- [52] See Supplemental Material at <http://link.aps.org/supplemental/10.1103/PhysRevB.107.L241405> for steady-state solution of density matrix, effective master equation, correlation functions under canonical transformations, beyond the rotating-wave approximation, quantum correlation and quantum entanglement, and collective quantum correlation. The Supplemental Material also contains Refs. [83–86].
- [53] N. Bogoljubov, V. V. Tolmachev, and D. Širkov, A new method in the theory of superconductivity, *Fortschr. Phys.* **6**, 605 (1958).
- [54] K. Svovil, Squeezed Fermion States, *Phys. Rev. Lett.* **65**, 3341 (1990).
- [55] R. Sánchez, G. Platero, and T. Brandes, Resonance Fluorescence in Transport through Quantum Dots: Noise Properties, *Phys. Rev. Lett.* **98**, 146805 (2007).
- [56] R. Sánchez, G. Platero, and T. Brandes, Resonance fluorescence in driven quantum dots: Electron and photon correlations, *Phys. Rev. B* **78**, 125308 (2008).
- [57] C. Xu and M. G. Vavilov, Full counting statistics of photons emitted by a double quantum dot, *Phys. Rev. B* **88**, 195307 (2013).

- [58] T. Frey, P. J. Leek, M. Beck, A. Blais, T. Ihn, K. Ensslin, and A. Wallraff, Dipole Coupling of a Double Quantum Dot to a Microwave Resonator, *Phys. Rev. Lett.* **108**, 046807 (2012).
- [59] H. Toida, T. Nakajima, and S. Komiyama, Vacuum Rabi Splitting in a Semiconductor Circuit QED System, *Phys. Rev. Lett.* **110**, 066802 (2013).
- [60] M. Kulkarni, O. Cotlet, and H. E. Türeci, Cavity-coupled double-quantum dot at finite bias: Analogy with lasers and beyond, *Phys. Rev. B* **90**, 125402 (2014).
- [61] Y.-Y. Liu, K. D. Petersson, J. Stehlik, J. M. Taylor, and J. R. Petta, Photon Emission from a Cavity-Coupled Double Quantum Dot, *Phys. Rev. Lett.* **113**, 036801 (2014).
- [62] Y.-Y. Liu, J. Stehlik, C. Eichler, M. Gullans, J. M. Taylor, and J. Petta, Semiconductor double quantum dot micromaser, *Science* **347**, 285 (2015).
- [63] S. Tarucha, D. G. Austing, T. Honda, R. J. van der Hage, and L. P. Kouwenhoven, Shell Filling and Spin Effects in a Few Electron Quantum Dot, *Phys. Rev. Lett.* **77**, 3613 (1996).
- [64] T. Oosterkamp, T. Fujisawa, W. van der Wiel, K. Ishibashi, R. Hijman, S. Tarucha, and L. P. Kouwenhoven, Microwave spectroscopy of a quantum-dot molecule, *Nature (London)* **395**, 873 (1998).
- [65] T. Fujisawa, T. H. Oosterkamp, W. G. Van der Wiel, B. W. Broer, R. Aguado, S. Tarucha, and L. P. Kouwenhoven, Spontaneous emission spectrum in double quantum dot devices, *Science* **282**, 932 (1998).
- [66] W. G. Van der Wiel, S. De Franceschi, J. M. Elzerman, T. Fujisawa, S. Tarucha, and L. P. Kouwenhoven, Electron transport through double quantum dots, *Rev. Mod. Phys.* **75**, 1 (2002).
- [67] S. M. H. Rafsanjani, M. Mirhosseini, O. S. Magaña-Loaiza, B. T. Gard, R. Birrittella, B. Koltjenbah, C. Parazzoli, B. A. Capron, C. C. Gerry, J. P. Dowling *et al.*, Quantum-enhanced interferometry with weak thermal light, *Optica* **4**, 487 (2017).
- [68] Y. Zhai, F. E. Becerra, J. Fan, and A. Migdall, Direct measurement of sub-wavelength interference using thermal light and photon-number-resolved detection, *Appl. Phys. Lett.* **105**, 101104 (2014).
- [69] G. Harder, D. Mogilevtsev, N. Korolkova, and C. Silberhorn, Tomography by Noise, *Phys. Rev. Lett.* **113**, 070403 (2014).
- [70] A. Jechow, M. Seefeldt, H. Kurzke, A. Heuer, and R. Menzel, Enhanced two-photon excited fluorescence from imaging agents using true thermal light, *Nat. Photonics* **7**, 973 (2013).
- [71] A. Gatti, E. Brambilla, M. Bache, and L. A. Lugiato, Ghost Imaging with Thermal Light: Comparing Entanglement and Classical Correlation, *Phys. Rev. Lett.* **93**, 093602 (2004).
- [72] H. A. M. Leymann, C. Hopfmann, F. Albert, A. Foerster, M. Khanbekyan, C. Schneider, S. Höfling, A. Forchel, M. Kamp, J. Wiersig, and S. Reitzenstein, Intensity fluctuations in bimodal micropillar lasers enhanced by quantum-dot gain competition, *Phys. Rev. A* **87**, 053819 (2013).
- [73] C. Redlich, B. Lingnau, S. Holzinger, E. Schlottmann, S. Kreinberg, C. Schneider, M. Kamp, S. Höfling, J. Wolters, S. Reitzenstein, and K. Lüdge, Mode-switching induced superthermal bunching in quantum-dot microlasers, *New J. Phys.* **18**, 063011 (2016).
- [74] M. Fanaei, A. Foerster, H. A. M. Leymann, and J. Wiersig, Effect of direct dissipative coupling of two competing modes on intensity fluctuations in a quantum-dot-microcavity laser, *Phys. Rev. A* **94**, 043814 (2016).
- [75] H. A. M. Leymann, D. Vorberg, T. Lettau, C. Hopfmann, C. Schneider, M. Kamp, S. Höfling, R. Ketzmerick, J. Wiersig, S. Reitzenstein, and A. Eckardt, Pump-Power-Driven Mode Switching in a Microcavity Device and Its Relation to Bose-Einstein Condensation, *Phys. Rev. X* **7**, 021045 (2017).
- [76] T. Lettau, H. A. M. Leymann, B. Melcher, and J. Wiersig, Superthermal photon bunching in terms of simple probability distributions, *Phys. Rev. A* **97**, 053835 (2018).
- [77] E. Schlottmann, M. von Helversen, H. A. M. Leymann, T. Lettau, F. Krüger, M. Schmidt, C. Schneider, M. Kamp, S. Höfling, J. Beyer, J. Wiersig, and S. Reitzenstein, Exploring the Photon-Number Distribution of Bimodal Microlasers with a Transition Edge Sensor, *Phys. Rev. Appl.* **9**, 064030 (2018).
- [78] M. Schmidt, I. H. Grothe, S. Neumeier, L. Bremer, M. von Helversen, W. Zent, B. Melcher, J. Beyer, C. Schneider, S. Höfling, J. Wiersig, and S. Reitzenstein, Bimodal behavior of microlasers investigated with a two-channel photon-number-resolving transition-edge sensor system, *Phys. Rev. Res.* **3**, 013263 (2021).
- [79] L. Mandel and E. Wolf, *Optical Coherence and Quantum Optics* (Cambridge University Press, Cambridge, 1995).
- [80] T.-C. Wei and P. M. Goldbart, Geometric measure of entanglement and applications to bipartite and multipartite quantum states, *Phys. Rev. A* **68**, 042307 (2003).
- [81] L. Amico, R. Fazio, A. Osterloh, and V. Vedral, Entanglement in many-body systems, *Rev. Mod. Phys.* **80**, 517 (2008).
- [82] R. Horodecki, P. Horodecki, M. Horodecki, and K. Horodecki, Quantum entanglement, *Rev. Mod. Phys.* **81**, 865 (2009).
- [83] M. O. Scully and M. S. Zubairy, *Quantum Optics* (Cambridge University Press, Cambridge, England, 1997).
- [84] M. Hillery and M. S. Zubairy, Entanglement Conditions for Two-Mode States, *Phys. Rev. Lett.* **96**, 050503 (2006).
- [85] M. Hillery and M. S. Zubairy, Entanglement conditions for two-mode states: Applications, *Phys. Rev. A* **74**, 032333 (2006).
- [86] S. Agarwal, S. M. Hashemi Rafsanjani, and J. H. Eberly, Tavis-Cummings model beyond the rotating wave approximation: Quasidegenerate qubits, *Phys. Rev. A* **85**, 043815 (2012).